The *N,N,N*-trimethylammonium moiety as tetrel bond donor site: crystallographic and computational studies

Received 00th January 20xx,
Accepted 00th January 20xx

DOI: 10.1039/x0xx00000x

Andrea Daolio,[a] Erna K. Wieduwilt,[b,c] Andrea Pizzi,[a*] Alessandro Genoni,[b*] Giuseppe Resnati,[a] Giancarlo Terraneo[a*]

Five structures bearing the *N,N,N*-trimethylammonium unit have been investigated to address the ability of the N^+–CH_3 unit to function as a tetrel bond donor site. Charged and neutral electron density donors display close contacts with different carbon atoms of methyl groups on the ammonium moiety. The Hirshfeld atom refinement (HAR) technique was used on selected structures to accurately and precisely determine the hydrogen atom positions and, consequently, to get better insights into the N^+-C···Nu (Nu= nucleophile) interactions occurring in the crystals. In particular, the performed analyses highlighted specific geometrical features of the moieties involved in the interactions and allowed to distinguish between tetrel and hydrogen bonds.

Introduction

Biological phenomena, materials properties, and chemical and biochemical reactions are deeply connected to non-covalent interactions.[1–4] In fact, in recent years, a large number of detailed experimental and computational works focused on understating and exploiting the attracting interactions promoted by various elements of the periodic table.[5–13]

It is known that the electron density distribution in a covalently bonded atom is anisotropic and that, on its surface, areas of lower and higher electron density can be present. Areas of reduced electron density are named σ-holes if localized approximately along the axis of covalent σ bond(s), while they are called π-holes if they appear above and below the plane of covalent π bond(s). The attractive interactions between these areas and electron density donor sites (such as neutral atoms with lone pairs, anions or π-systems) are correspondingly called σ-hole[14] or π-hole bondings.[15]

The mapping of areas of reduced electron density and the analysis of the specific short contacts formed by those areas were instrumental in the identification of some characteristic features of the Halogen Bond (HaB)[16], Chalcogen Bond (ChB)[17], Pnictogen Bond (PnB)[15,16] and Tetrel Bond (TtB).[17]

Carbon, the least polarizable tetrel atom, can possess both σ and π holes, and it can give rise to both σ-hole and π-hole interactions. However, the majority of the investigations discussing supramolecular entities assembled via carbon centered TtBs involve sp^2-hybidized carbon atoms and are discussed in term of π-holes interactions.[18–20] Studies on the formation of adducts promoted by C(sp^3)···Nu (Nu=nucleophile) attractive interactions are less numerous and are frequently limited to computational analyses[21–24] and crystallographic data mining research. [25,26]

Among other experimental findings on C(sp^3) moieties acting as TtB donors[27], some of us have recently reported the formation of tetrel bonded adducts by a small library of 5,5-dihalobarbituric acid derivatives where the C···O contact was a key supramolecular synthon in the stabilization of all crystal lattices.[28] Interestingly, upon the replacement of the two geminal hydrogen atoms on the barbituric acid ring with F/Cl/Br atoms, the carbon σ-holes became more effective in favoring the approach of an oxygen atom (namely the formation of the TtB) with the CF_2 moiety being the best TtB donor.

It is known that strong electron withdrawing groups σ-bonded to halogen/chalcogen/pnitogen/tetrel atoms increase the ability of the Ha/Ch/Pn/Tt donor atoms to accept electron density and thus to form shorter and stronger σ-hole interactions.[29–34]

In this context and with the aim to assess the ability of electron-withdrawing groups to promote σ-holes on a sp^3-hybridized carbon atoms, we directed our attention to the *N,N,N*-trimethylammonium moiety.

Ammonium groups have very high Hammet substituents constants and show higher electron-withdrawing ability than fluorides, cyano or nitro groups,[35] three functionalities which are frequently used to promote σ-holes formation. Moreover, ammonium residues are routinely employed as “active units” in biochemistry,[36] organic[37] and supramolecular chemistry.[38]

For instance, the *N,N,N,N′,N′,N′*-Hexamethylhexane-1,6-diaminium (also commonly known as hexamethonium) is a well-known compound acting as blocking agent of the nicotinic receptors and it was also studied as an effective compound for the cholinergic control of the neocortical output neurons.[39,40] Associated studies highlighted that the interactions between the trimethylammonium heads and electron rich units in the protein receptors were key factors in the regulation of many functions in living systems.[41]

In addition, the hexamethonium moiety has been also exploited in the field of crystal engineering where it was used to form

[a] *Department of Chemistry, Materials and Chemical Engineering “Giulio Natta”, Politecnico di Milano, Via L. Mancinelli 7, I-20131 Milan, Italy. E-mail: andrea.pizzi@polimi.it and giancarlo.terraneo@polimi.it*

[b] *Université de Lorraine & CNRS, Laboratoire de Physique et Chimie Théoriques (LPCT), UMR CNRS 7019, 1 Boulevard Arago, F-57078 Metz, France. E-mail: alessandro.genoni@univ-lorraine.fr*

[c] *Department of Physics, Chemistry and Pharmacy, University of Southern Denmark, Campusvej 55, 5320 Odense M, Denmark.*

Electronic Supplementary Information (ESI) available: Crystallographic details of **1**-**5**, Cambridge Structural Database Search and Fundaments of Hirshfeld Atom Refinement. See DOI: 10.1039/x0xx00000x

functional crystalline architectures able to trap specific guest molecules.[38]

However, although largely used as an efficient supramolecular unit, so far a detailed investigation of the interaction profile of the trimethylammonium moiety ($N^+(CH_3)_3$) in term of TtBs has never been addressed in detail.[42–45] This lack of experimental findings could be possibly related to the fact that it is not trivial to distinguish between a TtB and a hydrogen bond (HB) when a $-CH_3$ moiety is the electron density acceptor site.[46]

In fact, on the one hand it is reasonable to imagine the formation of a σ-hole on carbon along the extension of the N^+-CH_3 bond and thus predict the formation of a TtB with a nucleophile, on the other hand it is not easy to reliably rule out the formation of HBs between methyl hydrogen(s) and the nucleophile due to the enhanced acidity of these hydrogen atoms.

Aiming to investigate this dual behaviour of the trimethylammonium moiety, we decided to analyse its interaction profile via a combination of experimental and computational approaches to dissect the role of TtB and HB in driving the formation of supramolecular adducts.

The *N,N,N,N',N',N'*-hexamethylhexane-1,6-diaminium was selected as molecular entity bearing the TtB donor moiety in relation to its functional relevance sketched above (Scheme 1).

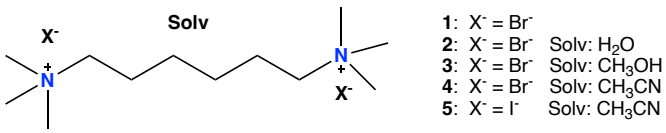

1: X^- = Br^-
2: X^- = Br^- Solv: H_2O
3: X^- = Br^- Solv: CH_3OH
4: X^- = Br^- Solv: CH_3CN
5: X^- = I^- Solv: CH_3CN

Scheme 1. Structural formulas of the investigated hexamethonium derivatives.

Initial single-crystal X-ray diffraction experiments displayed close and generally linear contacts between one (or more) C atom of the methyl(s) and halide anions or neutral electron rich molecules, highlighting the possible presence of a TtB. Since a tetrel bonded sp^3 carbon forms a pseudo-hypervalent state that roughly mimics the transition state of a nucleophilic substitution reaction and adopts a "flattened" conformation of the tetrahedral arrangement of the hydrogen atoms,[47,48] we decided to accurately determine the positions of the hydrogen atoms using Hirshfeld atom refinement (HAR).[49–53] HAR analysis is an emerging technique of quantum crystallography[54–56] that, using only X-ray diffraction data, enables to locate the position of hydrogen atoms with the same precision and accuracy that is usually attained through neutron diffraction measurements.[51]

The crystal structures obtained through HAR were afterwards analysed from the geometrical point of view and were used to perform quantum topological analyses to better characterize the interaction profile between the CH_3 units and the nucleophiles.[57–60]

Experimental methods

Materials.

All starting materials and reagents were purchased from commercial suppliers (Sigma Aldrich, TCI) and used without further purification.

Experimental Conditions.

Crystals **1-5** were obtained by slow evaporation in a clear borosilicate vial of solutions containing 0.1 mmol of 1,6 trimethylammonium hexane dibromide (**1-4**) and 1,6 trimethylammonium hexane diiodide (**5**). The structure of crystal **1**[61] was obtained by slow evaporation of a CH_2Cl_2 solution, crystals of **2**[62] were obtained from an H_2O solution, of **3** from a CH_3OH solution, of **4** and **5** from an acetonitrile solution. In all performed experiments, small needle-like crystals suitable for X-Ray diffraction were collected at the bottom of the vial. The single crystal data of all the structures displayed in this work were collected at Bruker SMART APEX II CCD area detector diffractometer at low temperature (see ESI). Data collection, unit cell refinement and data reduction were performed using Bruker SAINT.

Independent Atom Model Refinements.

The structures were solved by direct methods using SHELXT[63] and refined by full-matrix least-squares on F^2 with anisotropic displacement parameters for the non-H atoms using SHELXL-2016/6. Absorption correction was performed on the basis of a multi-scan procedure using SADABS. Structural analysis was aided by use of the program PLATON.[64] The hydrogen atoms were calculated in ideal positions with isotropic displacement parameters set to $1.2xU_{eq}$ of the attached atom.

Hirshfeld atom refinements.

For crystals **1**, **2** and **5**, for which quality and resolution of the collected X-ray data are sufficiently high, Hirshfeld Atom Refinements were carried out exploiting the software *Tonto*[65]. All the HARs started from crystal structures resulting from preliminary independent atom model (IAM) refinements performed through SHELXL (see above). The *ab initio* electron densities used in the Hirshfeld atom refinements were calculated at Density Functional Theory (DFT) level with hybrid functional B3LYP and basis-set DGDZVP.[66] In crystals **1** and **2**, only half of hexamethonium is included in the asymmetric unit. Therefore, exploiting the existing inversion centre, the molecule was grown and the whole hexamethonium was considered in the computations underlying the HARs. In crystal **2**, the above-mentioned inversion centre also connects two solvent water molecules, which were also consequently included in the DFT calculations. For crystal **5**, the whole hexamethonium forms the asymmetric unit and only one solvent acetonitrile molecule, namely the one closest to hexamethonium, was included in the DFT computations. In addition to solvent molecules (where they were present), also the surrounding nucleophiles (Nu) were necessarily taken into account in the *ab initio* calculations underlying the performed HARs. For this reason, for all crystal structures refined through HAR (i.e., **1**, **2**, and **5**) two halide ions were also explicitly considered in the computations. Finally, in order to account for the effects of the crystal environment, the

central systems selected for the *ab initio* calculations (i.e., whole hexamethonium, solvent molecule(s) (when present) and halide anions), were embedded in clusters of atomic charges and dipoles placed on all the atoms of the surrounding moieties having at least one atom within a radius of 8 Å from the central system. For the sake of completeness, it is also worth pointing out that all HARs were performed against the structure factor amplitudes F using an F > 3σ(F) cutoff. Furthermore, for the Hirshfeld atom refinement of crystal **2**, it was necessary to fix the positions and the ADPs of the hydrogen atoms in the water molecules to the values obtained from the preliminary IAM refinement performed with SHELXL.

Computational details.

For each crystal structure obtained from the Hirshfeld atom refinements, we considered the electron densities resulting from DFT calculations at B3LYP/DGDZVP level performed with the quantum chemistry package Gaussian09.[61] These electron distributions were used to carry out Quantum Theory of Atoms In Molecules (QTAIM)[67] and Non-Covalent Interaction[53-56] (NCI) analyses with the final goal of detecting or not the presence of tetrel bond interactions in the refined structures. The QTAIM analyses were performed using the software AIMAll,[68] while the NCI computations were carried out exploiting the program NCIPLOT-3.0[58] and adopting the default options.

Results and Discussion

1. Crystal structures description

The hexamethonium structures and the contacts between carbon atoms and nucleophiles in structures **1-5** are given in Figure 1. A more detailed description is given below with a table encompassing the geometrical features of the analysed contacts (Table 1).

N,N,N,N′,N′,N′-Hexamethylhexane-1,6-diaminium dibromide (**1**)[61] crystallizes in $P2_1/c$ space group where the hexamethonium chain adopts a linear conformation. The crystal packing of **1** appears, along the crystallographic *b*-axis, as a layered structure where hexamethonium units and bromide anions alternate. The cations and the anions layers interact thanks to several HBs occurring between the bromide anions and the hydrogen atoms of the $N^+–CH_3$ or $N^+–CH_2–$ moieties.
Two carbon atoms belonging to different methyl groups display linear N-C···Br contacts with different bromide anions. These interactions can be considered as weak TtBs despite being very close the sum of the respective van der Waals and anionic radii (as indicated by the normalized contact (Nc)[§] reported in Figure 1).

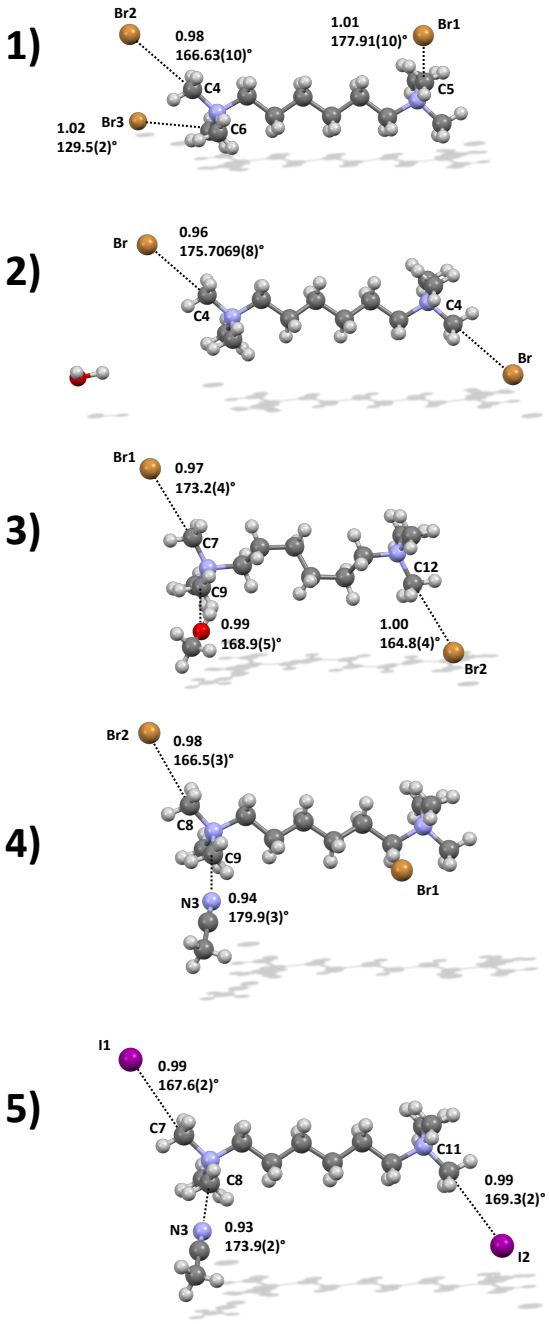

Figure 1. Ball and stick representation (Mercury) of structures of hexamethonium derivatives **1-5**. Close C···Nu contacts are represented with black dotted lines. N–C···Nu angles (°) and Nc values of C···Nu separations (IAM refinements) are given near the dotted lines. Colour code: *whitish* hydrogen, *grey* carbon, *light blue* nitrogen, *red* oxygen, *brown* bromine, *purple* iodine.

The geometrical parameters are the following: the first contact involves C5 and Br1 with C···Br distance of 3.7006(16) Å (Nc 1.01) and N–C···Br angle of 177.91(10)°, while the second contact involves C4 and Br2 (the bromide anion labelled as Br2 is the symmetry generated of $Br1_{(x,0.5-y,0.5+z)}$) with C···Br distance of 3.5925(16) Å (Nc 0.98) and N–C···Br angle of 166.63(10)°. Both contacts have Nc value close to 1, but, notably, the directionality of the angles between donor and acceptor unit

agree with the distinctive feature of the σ-hole bonding interactions.

When crystallized from water, *N,N,N,N′,N′,N′*-hexamethylhexane-1,6-diaminium dibromide crystallizes in $P2_1/c$ space group as the solvate **2.**[62] In this crystal the hexyl chain adopts a slightly distorted *all-trans* conformation and the bromide anion establishes a close contact with the C atom of one N^+–CH_3 unit. Specifically, the C4···Br distance is 3.4922(14) Å (Nc 0.96) and the N–C4···Br angle is 175.69(8)°, namely the geometric features of the interaction are those typical for a TtB. In addition, the bromide anion also forms many HBs with H atoms belonging to water molecules and to CH_3 and CH_2 groups of adjacent hexamethonium units. Waved and alternating layers of hexamethonium cations and bromide anions plus water molecules are present in the crystal packing as apparent when viewing the crystal along the *a*-axis.

When crystallized from methanol, *N,N,N,N′,N′,N′*-hexamethylhexane-1,6-diaminium dibromide crystalizes in $P2_1/n$ space group as the solvate **3**. Hexyl chains in this crystal show the presence of two *gauche* arrangements, different from all other hexamethonium derivatives discussed in this paper wherein chains are in an *all-trans* conformation. Similar to **2**, in **3** the bromide anion Br1 forms several hydrogen bonds with –CH_3 and –CH_2– moieties of the cation and a short contact with a C atom of the methyl group of the ammonium head (the C7···Br1 distance is 3.534(8) Å (Nc 0.97), the N1–C7···Br1 angle is 173.2(4)°). Similarly, the anion Br2 engages in multiple HBs with the methanol molecule and two different hexamethonium units and forms a N–C···Br contact at the van der Waals distance which can be rationalized as a TtB (the C12···Br2 distance is 3.659(7) Å (Nc 1.00) and the N2–C12···Br2 angle is 164.8(4)°). Also, the methanol molecule forms several HBs and notably its oxygen atom displays a short N–CH_3···O contact which can be rationalized as a TtB (the C9···O1 distance is 3.215(9) Å (Nc 0.99), the N1–C9···O1 angle is 168.9(5)° (Figure 1).

When crystallized from acetonitrile, *N,N,N,N′,N′,N′*-hexamethylhexane-1,6-diaminium dibromide crystallizes in $P2_1/c$ space group as solvate **4**. In this structure, the hexamethonium units adopt a linear conformation. The interaction pattern of bromide anions recalls those observed in the previous crystal structures. Both bromide anions show multiple HBs with the CH_3 and CH_2 moieties of hexamethonium units and with the CH_3 of the acetonitrile. One of these bromide anions (Br2) also forms a short contact with the carbon atom of one ammonium methyl (the C8···Br2 distance is 3.596(5) Å (Nc 0.98) and the N1–C8···Br2 angle is 166.5(3)°). Notably, in this crystal the acetonitrile molecule displays a very linear contact with the carbon atom of one ammonium methyl and the geometrical parameters are typical for a TtB (the C9···N3 distance is 3.065(5) Å (Nc 0.94) and the N1–C9···N3 angle is 179.9(3)°).

When crystallized from acetonitrile. *N,N,N,N′,N′,N′*-hexamethylhexane-1,6-diaminium diiodide crystallizes in $P2_1/n$ space group. Similar to **4**, the compound crystallizes as the solvate **5** and the acetonitrile molecule is engaged in a short and linear contact with the carbon atom of an ammonium methyl (the C8···N3 distance is 3.016(6) Å (Nc: 0.93) and the N2–C8···N3 angle is 173.9(2)°). The two iodide anions form multiple HBs with hydrogen atoms of hexamethonium units and they both give contacts with ammonium methyl groups having Nc values close to 1 (the C11···I2 and C7···I1 distances are both 3.816(4) Å (Nc 0.99), while the N1–C11···I2 and N2–C7···I1 angles are 169.3(2)° and 167.6(2)°, respectively).

Overall, all five crystal structures display close contacts between carbon atoms of ammonium methyl groups and electron density donor moieties (both neutral and anionic, Table 1). These contacts could be described as attractive C···nucleophile contacts, namely TtBs, but could also be considered short C···nucleophile contacts resulting from attractive H···nucleophile contacts, namely HBs, involving the positively charged methyl hydrogen atoms. The crystallographic analyses described above can hardly discriminate between the two possibilities. Therefore, Hirshfeld atom refinements were performed on selected structures to determine with higher accuracy and precision the positions of the hydrogen atoms and, consequently, to acquire a better understanding of the actual binding site(s) of the ammonium methyl groups responsible for the short contacts with nucleophiles. In fact, various studies correlated the W–C···Nu *vs.* C–H···Nu angles (with W as the electron withdrawing group responsible for carbon and hydrogen electrophilicity) with the TtB *vs.* HB origin of the methyl-nucleophile short contact(s).[39,42]

Table 1. Geometrical features of C···Nu close contacts in structures **1**-**5** from IAM refinement and HAR refinement [in parenthesis].

Structure	Nu	C···Nu distance (Å)	N^+–C···Nu angle (°)
1	Br1[′]	3.7006(16)	177.91(10)
		[3.7056(13)]	[177.99(8)]
	Br2[′]	3.5925(16)	166.63(10)
		[3.5924(16)]	[166.77(9)]
2	Br[′]	3.4922(14)	175.69(8)
		[3.4934(14)]	[175.56(8)]
3	Br1	3.534(8)	173.2(4)
	Br2	3.659(7)	164.8(4)
	O1	3.215(9)	168.9(5)
4	N3	3.065(5)	179.9(3)
	Br2	3.596(5)	166.5(3)
5	N3[′]	3.016(6)	173.9(2)
		[3.023(6)]	[174.0(3)]
	I1[′]	3.816(4)	167.6(2)
		[3.826(4)]	[167.5(2)]
	I2[′]	3.816(4)	169.3(2)
		[3.811(4)]	[169.7(3)]

2. Hirshfeld Atom Refinement

As already mentioned above, when the resolution and the quality of the experimental X-ray diffraction data were sufficiently high, additional Hirshfeld atom refinements were performed, with the final goal of establishing more accurately and precisely the positions of hydrogen atoms. This is particularly important for a reliable identification of the TtBs involving the N^+–CH_3 moiety. In fact, the accurate determination of the hydrogen atom positions in the methyl

groups would in principle allow to establish with a higher confidence if the electron density donor atoms attractively interact with the methyl carbon atom rather than with the methyl hydrogen atoms.

As expected, the HARs provide geometrical features that are slightly different from those resulting from the traditional IAM refinements described above (Table 1).

The two C···Br interactions in crystal **1** seem to be more linear after HAR refinement than after IAM refinement. HAR uses the same atom numbering of IAM and an apex is added (e.g., Br1 in IAM is encoded Br1' in HAR); the N1'–C5'···Br1' angle is 177.99(8)° and the N1'–C4'···Br2' is 166.77(9)° (the values of the respective angles after IAM refinement were 177.91(10)° and 166.63(10)°). The new refinement seems to have an impact also on C···Br distances, but the change is of lower entity (Table 1). On the contrary, HAR determines positions of methyl hydrogen atoms, which are significantly different from those previously obtained through IAM refinements. In general, C–H bonds become longer in all the structures treated with HAR. Specifically, in **1**, the geometrical features of the hydrogen atoms of the two tetrel bonded methyl groups reflect a different interaction profile with the bromide anion. When the electron density donor site is Br1', the three H···Br1' distances are 3.498(17) Å (H_a), 3.546(17) Å (H_b), and 3.559(17) Å (H_c) (Table 2). The values of $N'^{+}-C'-H$ angles for all the three hydrogen atoms are slightly lower than the IAM values (mean angle 107.7° *vs.* 109.5°), thus HAR indicates a flattening of the methyl hydrogen atoms compared to the ideal angle assumed in the IAM. In addition, the values of the C'–H···Br1' angles for this methyl group are similar and close to 90° (Table 2). These geometrical parameters of the H atoms on the TtB donor site C5' suggest the absence of HBs and, consequently, the rationalization of the interaction as a TtB.

The second methyl group, where the TtB donor site is C4', presents a different geometrical arrangement of the H atoms. The three H···Br2' distances are not similar to each other (3.199(16) Å for H_d, 3.456(17) Å for H_e and 3.621(18) Å for H_f; see again Table 2). This is particularly evident for the one that involves atom H_d, which is significantly closer to the bromide anion than the others. Although the $N'^{+}-C'-H$ angles for this methyl group do not necessarily show large deviation from those obtained for the C5'···Br1' interaction, it is worth pointing out that angle $N^{+}-C4'-H_d$ is slightly wider than the other two. Finally, if the C4'–H···Br2'angles are analysed, it is possible to notice how the C4'-H_d···Br2' angle is much closer to "linearity" (102.5(9)°) than the other two cases (88.8(9)° and 80.3(10)° respectively, Table 2). This spatial orientation of the H atoms is quite different from the one observed for the C5'···Br1' interaction and may suggest an attractive contribution of hydrogen atom H_d in promoting the interaction between C4' and the electron density donor site Br2'.

For comparison, it is interesting to analyse the third methyl group that does not show any close contact between a bromide anion and the carbon atom, but a very clear hydrogen bond with another adjacent halide anion (for the sake of this discussion here indicated as Br3'). In this case, the distance of Br3' from the carbon is 3.7281(16) Å and the $N^{+}-C6'\cdots Br3'$ angle is 129.54(9)°, strongly consistent with an HB between one of the hydrogen atoms (H_g) and the bromide anion. It is clear that the geometrical values of this case are much more similar to the interaction involving Br2' than to the one involving Br1'. In fact, the C6'–H_g···Br3'angle is much closer to 180° than the others (interaction motives are depicted in Figure 2).

From the HAR analysis it is then possible to conclude that the C5'···Br1' contact could be considered as a TtB interaction while the C4'···Br2' contact is more likely a HB contact between H_d and Br2' with a possible contribution of TtB interaction.

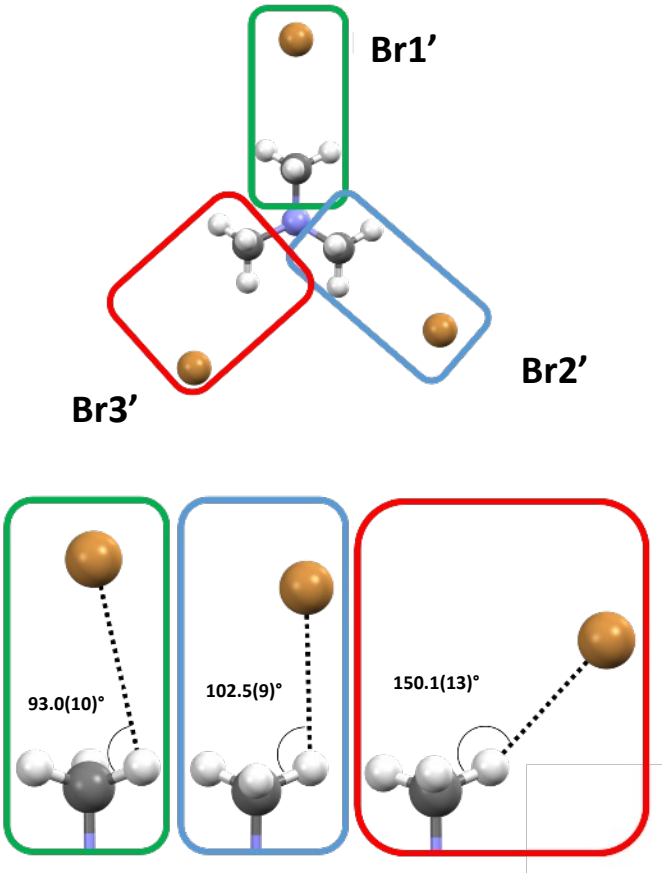

Figure 2. Different interactions in the HAR refined crystal structure **1**. The interactions are depicted with the nucleophile approaching the carbon atom. The associated Br···H–C angles are reported at the bottom of the figure.

Concerning crystal **2**, it is clear that the interaction between the bromide anion and the C atom of the methyl group should be described as a TtB. In the analysed HAR structure the C4'···Br' separation distance is 3.4934(14) Å (Nc value lower than 1) and $N^{+}-C4'\cdots Br'$ angle is very linear (175.56(8)°). Additionally, the better refinement of the hydrogen positions reveals that the positions of those atoms are consistent with the geometrical features already highlighted in the discussion of the HAR structure **1**. In fact, in structure **2**, the distances between Br' and the hydrogen atoms are 3.253(15) Å (H_a), 3.268(15) Å (H_b), 3.384(13) Å (H_c) and the $C4'-H\cdots Br'$ angles are 93.9(9)°, 94.0(10)° and 86.8(7)°, respectively, which mirror the values observed in the C5'···Br1' TtB interaction in **1**.

Finally, crystal **5** presents multiple TtB interactions, all of them described in Table 2. First, we discuss the interaction taking place between a carbon atom (C8') of hexamethonium and the nitrogen atom of an acetonitrile solvent molecule. All the geometrical features of the C8'···N3' interaction are consistent with a TtB contact where the electron density donor site (N3') approaches the C atom on the trajectory of an N^+–C bond with a C8'···N3' distance lower than the sum of the van der Waals radii (3.023(6) Å) and an $N^+ - C8'\cdots N3'$ angle close to 180° (174.0(3)°). This structural motif is similar to the TtB contacts described in the other structures. In fact, the C'–H···N' angles are close to 90° showing a "flat" disposition of the methyl hydrogens. The close contact between anion I2' and carbon atom C11' on the methyl group seems to unequivocally be a TtB. In this case, the N^+–C–H angles are remarkably smaller than those observed for the other methyl groups, and, more importantly, much closer to planarity than the others (Table 2). Instead, the other iodide anion (I1') is in a situation similar to the one seen in structure **1** for site Br2', where a strong contribution of an HB is detected. In fact, the C7'–H_d···I1'angle of 105.0(3)° is consistent with an HB between I1' and H_d

Table 2. Geometrical features of the hydrogen atoms in the HAR-refined structures

Structure	Nu	C-H	H···Nu distance (Å)	N^+–C–H angle (°)	C–H···Nu angle (°)
1	Br1'	C5'–H_a	3.498(17)	107.5(9)	93.0(10)
		C5'–H_b	3.546(17)	107.9(9)	90.4(10)
		C5'–H_c	3.559(17)	107.2(9)	89.8(10)
	Br2'	C4'–H_d	3.199(16)	108.1(9)	102.5(9)
		C4'–H_e	3.456(17)	106.4(9)	88.8(9)
		C4'–H_f	3.621(18)	107.8(10)	80.3(10)
	Br3'	C6'–H_g	2.781(17)	109.8(9)	150.1(13)
		C6'–H_h	3.919(17)	106.3(9)	71.9(8)
		C6'–H_i	4.174(16)	106.1(9)	57.5(8)
2	Br'	C4'–H_a	3.253(15)	108.7(8)	93.9(9)
		C4'–H_b	3.268(15)	110.1(9)	94.0(10)
		C4'–H_c	3.384(13)	109.1(7)	86.8(7)
5	N3'	C8'–H_a	2.76(3)	108.7(18)	92.0(19)
		C8'–H_b	2.87(4)	109.1(18)	87.1(19)
		C8'–H_c	2.98(4)	107.1(2)	82.3(2)
	I1'	C7'–H_d	3.40(5)	109.8(3)	105.0(3)
		C7'–H_e	3.65(4)	107.3(2)	89.8(3)
		C7'–H_f	3.89(4)	106.4(2)	78.5(2)
	I2'	C11'–H_g	3.46(5)	106.7(2)	98.0(3)
		C11'–H_h	3.73(5)	103.3(3)	86.9(3)
		C11'–H_i	3.83(4)	106.1(2)	81.1(2)

3. Topological analyses.

To get further insights into the nature of the above-mentioned contacts and to better describe the tetrel bond interactions, NCI and QTAIM analyses were carried out exploiting the B3LYP/DGDZVP electron densities associated with the experimental structures. In these analyses, we considered only the obtained HAR structures since for them we have reliable positions of the hydrogen atoms.

The nature of the hexamethonium/nucleophile contacts was initially investigated by means of non-covalent interaction (NCI) analyses. The obtained reduced density gradient isosurfaces resulting from the NCI computations are reported in Figure 3.

In compound **1**, Br1' establishes an interaction with the closest methyl carbon atom. This is clearly supported by the HAR refinement of the structures. Also in crystal **2**, the reduced density gradient isosurfaces indicate the presence of direct C4'···Br' tetrel bond interaction, mirroring and confirming again the results of the Hirshfeld atom refinements. Finally, for crystal **5**, always in agreement with the previous structural observations, the NCI surfaces indicate the presence of a non-covalent interaction between acetonitrile and hexamethonium as well as presence of iodine/hexamethonium contacts. However, in this case, the NCI analysis does not allow to accurately discriminate if the latter are mainly due to iodine-carbon interactions (namely TtB) or to iodine/hydrogen interactions. Therefore, to answer these questions and to get more insights into the nature of the observed interactions, we decided to resort to a QTAIM analysis, whose results are presented and discussed in the next paragraphs for all the analysed crystal structures.

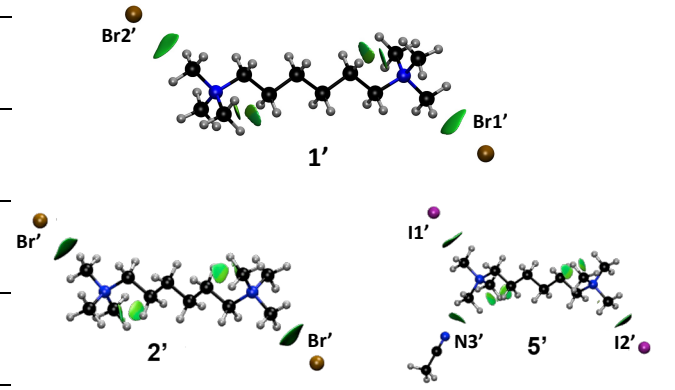

Figure 3. Reduced density gradient isosurfaces (s=0.5 a.u.) obtained from the NCI analyses performed on the HAR structures of (a) crystal **1**, (b) crystal **2** and (c) crystal **5**. The NCI analyses are based on electron densities resulting from DFT calculations at B3LYP/DGDZVP level.

In Table 3 we present the results of the topological analysis. In addition, for each detected bond critical point (bcp), we also reported the corresponding topological properties (Table 3). For both crystals **1** and **2,** it is possible to observe the presence of a bond path and one bond critical point between the bromine atom (Br1') and the respective carbon atom of the methyl group, as predicted by the analysis of the HAR structure. Therefore, as already expected from the geometrical and NCI analyses, the topological properties of the electron density confirm the presence of a TtB interaction between Br' and C5' (crystal **1**) as well as between Br' and C4' (crystal **2**).

Table 3. Bond critical points and associated topological properties corresponding to tetrel and hydrogen bonds for the B3LYP/DGDZVP electron densities computed on the crystal structures resulting from Hirshfeld atom refinements.

Structure	Atoms	ρ_{bcp} (ebohr^{-3})	$\nabla^2\rho_{bcp}$ (ebohr^{-5})	G_{bcp} (hartree bohr^{-3})	V^{bcp} (hartree bohr^{-3})	$\lvert V_{bcp}\rvert/G_{bcp}$	BD	DI
1	Br1'···C5'	0.006	0.015	0.0031	-0.0024	0.78	0.12	0.06
2	Br'···C4'	0.008	0.023	0.0049	-0.0040	0.81	0.12	0.08
5	I1'···Hd	0.007	0.018	0.0036	-0.0028	0.77	0.12	0.05
	I2'···C11'	0.007	0.016	0.0034	-0.0026	0.78	0.11	0.07
	N3'···C8'	0.008	0.035	0.0069	-0.0051	0.74	0.21	0.04

Finally, for crystal **5**, a bond path between iodine atom I1' and methyl hydrogen H_d, and another one between iodine atom I2' and the closest methyl carbon C11'. These results highlight how the contact involving I2' is a TtB while the one involving I1' is a HB. In addition, in **5**, the analysis also reveals the presence of a bond critical point between the nitrogen atom of the acetonitrile solvent molecule and methyl carbon C8' of one of the hexamethonium heads, which is consistent with the structural observations discussed above and the classification of the contact as TtB.

Further analysing the results of QTAIM (Table 3), for the detected C···Nu bond critical points (bcps), we can notice that all values of the electron density at the bcps (ρ_{bcp}) are quite small. However, we can also see that the interactions C4'···Br' and C11'···I2' in crystals **2** and **5** are characterized by ρ_{bcp} values that are slightly greater than the ρ_{bcp} value obtained for the C5'···Br1' contact in crystal **1**. These values suggest that the TtB contacts C4'···Br' and C11'···I2' in crystals **2** and **5**, respectively, are slightly stronger than the one detected in crystal **1**. Furthermore, we can observe that all the Laplacian values at the bond critical points ($\nabla^2\rho_{bcp}$) are positive, which allows us to classify the analysed interactions as closed-shell.[67] Moreover, the ratio between the absolute value of the potential energy density at the bond critical point (V_{bcp}) and the kinetic energy density at the bond critical point (G_{bcp}) (namely $\lvert V_{bcp}\rvert/G_{bcp}$) is always lower than 1. For this reason, following the classification proposed by Espinosa[69], all the detected (non-covalent) interactions can be also further identified as pure closed-shell interactions and therefore the bond degree (BD) parameter can be used as strength-index of the interactions (the stronger the interaction, the lower the BD value). Unlike the ρ_{bcp} values, the BD descriptor indicates that the three considered contacts are basically equivalent, with the C11'···I2' interaction in structure **5** (BD=0.11) only slightly stronger than C5'···Br1' and C4'···Br' in structures **1** and **2**, respectively (BD=0.12). However, it is worth noting that the trends observed for ρ_{bcp} are also confirmed by a third topological descriptor, namely the delocalization index (DI), which is a measure of the electrons shared between two atomic basins and generally correlates with bond order. In this case, the DI value associated with interaction C4'···Br' in **2** (DI=0.08) is greater than the one corresponding to contact C11'···I2' in **5** (DI=0.07), which is in turn greater than the DI value for the interaction C5'···Br1' in **1** (DI=0.06). Finally, concerning the interaction between the acetonitrile solvent molecule and hexamethonium in structure **5** (last line of Table 3), we observed that, although the ρ_{bcp} value of the associated bond critical point is comparable to the ones for C4'···Br' and C11'···I2' bcps in crystals **2** and **5**, respectively, the other two topological descriptors (BD and DI) indicate that this interaction is weaker than those involving halide anions.

The above described QTAIM analysis provided results of topological properties completely in line with those reported in previous investigations on tetrel bond interactions [23,70–72]and, above all, it allowed us to properly classify the contacts between electron density donors with different nature (neutral and charged) and carbon atoms on methyl groups of the hexamethonium dication. Specifically, some of the analysed interactions were tetrel bonds while others, classified as potential TtBs on the basis of the traditional crystal structure analysis, turned out to be probably more similar to HB interactions. Therefore, the proposed approach is a valuable protocol that can be used to distinguish situations where multiple electron density acceptor sites (namely C and H atoms) are in proximity with electron density donor units.

Conclusions

In the present paper, five crystal structures bearing the *N,N,N*-trimethylammonium unit have been investigated analysing the geometrical and topological features of the N^+– C···Nu (Nu=Nucleophile) interaction with the aim to address the ability of the C atom belonging to the N^+–CH_3 unit to form σ-hole interactions with different nucleophiles.

The identification of the N^+–C···Nu contacts has been initially performed on structures refined through the standard IAM approach. This analysis revealed that nucleophiles formed short contacts with the C atom of the N^+–CH_3 units; some contacts showed geometrical parameters consistent with tetrel bonds, (TtBs) while some others exhibited geometrical features which rather suggested the possible presence of hydrogen bonds (HBs).

To better characterize the interactions taking place in the structures and to clearly distinguish between a TtB or HB, a series of refinement and computational tools were used. First, when possible, the structures were refined using HAR allowing a more reliable description of the hydrogen atom positions. These refined models have shown how a more realistic positioning of the H atoms on the N^+–CH_3 units allowed a better description of the angles and thus a clearer distinction between TtB and HB. In fact, in the TtB interactions, the classical tetrahedral geometry of the H atoms on the N^+–CH_3 unit evolved towards a pseudo-trigonal bipyramid geometry with C−H···Nu angle values closer to 90°. Differently, when the interactions were HBs, one of the C−H···Nu angles showed a value higher than 100°, thus highlighting the contribution of H atom in the formation of the contact. This result is in agreement with previous findings on TtB interactions[32,73] and clearly supports the importance to locate the position of the hydrogen atoms on a TtB donor site unit showing how the geometrical features of the C–H···Nu angles can be used to distinguish between tetrel and hydrogen bonds.

In addition, the HAR structures were also used to further characterize the TtB interactions using the QTAIM and NCI computational tools. Especially the QTAIM analysis helped to distinguish TtBs from HBs. Furthermore, the analysis of the topological properties allowed us to estimate the strength of the TtB interactions, revealing trends consistent with the definition of σ-hole interactions.

Finally, here we have shown that N^+–CH_3 units can function as tetrel bond donor site both with charged and neutral electron density donor units. The Hirshfeld atom refinement technique is fundamental to determine the hydrogen atoms position accurately and precisely, and, consequently, to get more insights into the nature of the N^+–C···Nu interactions.

Overall, this work confirms the key role of TtB in stabilizing the supramolecular assembling of molecules bearing “TtB active” units and further highlights the implication that this non covalent interaction could have in different research fields such as organic chemistry[72] or biomolecules.[74]

Author Contributions

GR and GT designed the experiments. AD and AP performed the experiments. GT oversaw the crystallographic characterization. EW and AG performed and interpreted the HARs and the computational studies. GR, AD, AP, GT, EW and AG interpreted the results. All the authors wrote the paper.

Conflicts of interest

There are no conflicts to declare.

Notes and references

§ The normalized contact for an interaction between neutral atoms i and j is the ratio Dij/(rvdW,i+rvdW,j) wherein Dij is the experimental separation between i and j and rvdW,i and rvdW,j are the van der Waals radii of i and j, respectively.

1 B. L. Feringa, The Art of Building Small: From Molecular Switches to Motors (Nobel Lecture), *Angew. Chemie Int. Ed.*, 2017, **56**, 11060–11078.

2 R. W. Newberry and R. T. Raines, The n→π* Interaction, *Acc. Chem. Res.*, 2017, **50**, 1838–1846.

3 S. Varughese, Non-covalent routes to tune the optical properties of molecular materials, *J. Mater. Chem. C*, 2014, **2**, 3499–3516.

4 C. Yuan, W. Ji, R. Xing, J. Li, E. Gazit and X. Yan, Hierarchically oriented organization in supramolecular peptide crystals, *Nat. Rev. Chem.*, 2019, **3**, 567–588.

5 G. Cavallo, P. Metrangolo, T. Pilati, G. Resnati and G. Terraneo, Naming interactions from the electrophilic site, *Cryst. Growth Des.*, 2014, **14**, 2697–2702.

6 P. Song and H. Wang, High-Performance Polymeric Materials through Hydrogen-Bond Cross-Linking, *Adv. Mater.*, 2020, **32**, 1901244.

7 H. Schmidbaur and A. Schier, Aurophilic interactions as a subject of current research: an up-date, *Chem. Soc. Rev.*, 2012, **41**, 370–412.

8 R. M. Gomila and A. Frontera, Covalent and Non-covalent Noble Gas Bonding Interactions in XeFn Derivatives (n = 2–6): A Combined Theoretical and ICSD Analysis, *Front. Chem.*, 2020, **8**, 395.

9 A. Bauzá, I. Alkorta, J. Elguero, T. J. Mooibroek and A. Frontera, Spodium Bonds: Noncovalent Interactions Involving Group 12 Elements, *Angew. Chemie Int. Ed.*, 2020, **59**, 17482–17487.

10 A. Daolio, A. Pizzi, M. Calabrese, G. Terraneo, S. Bordignon, A. Frontera and G. Resnati, Molecular Electrostatic Potential and Noncovalent Interactions in Derivatives of Group 8 Elements, *Angew. Chemie Int. Ed.*, 2021, **60**, 20723–20727.

11 P. Politzer, J. S. Murray, T. Clark and G. Resnati, The σ-hole revisited, *Phys. Chem. Chem. Phys.*, 2017, **19**, 32166–32178.

12 P. Politzer and J. S. Murray, *Cryst.* , 2019, 9.

13 G. R. Desiraju, P. S. Ho, L. Kloo, A. C. Legon, R. Marquardt, P. Metrangolo, P. Politzer, G. Resnati and K. Rissanen, Definition of the halogen bond (IUPAC Recommendations 2013), *Pure Appl. Chem.*, 2013, **85**, 1711–1713.

14 C. B. Aakeroy, D. L. Bryce, G. R. Desiraju, A. Frontera, A. C. Legon, F. Nicotra, K. Rissanen, S. Scheiner, G. Terraneo, P. Metrangolo and G. Resnati, Definition of the chalcogen bond (IUPAC Recommendations 2019), *Pure Appl. Chem.*, 2019, **91**, 1889–1892.

15 S. Scheiner, The Pnicogen Bond: Its Relation to Hydrogen, Halogen, and Other Noncovalent Bonds, *Acc. Chem. Res.*, 2013, **46**, 280–288.

16 P. Scilabra, G. Terraneo, A. Daolio, A. Baggioli, A. Famulari, C. Leroy, D. L. Bryce and G. Resnati, 4,4’-Dipyridyl Dioxide·SbF<inf>3</inf> Cocrystal: Pnictogen Bond Prevails over Halogen and Hydrogen Bonds in Driving Self-Assembly, *Cryst. Growth Des.*, 2020, **20**, 916–922.

17 A. Bauzá, T. J. Mooibroek and A. Frontera, Tetrel Bonding Interactions, *Chem. Rec.*, 2016, **16**, 473–487.

18 H. B. Burgi, J. D. Dunitz and E. Shefter, Geometrical reaction coordinates. II. Nucleophilic addition to a carbonyl group, *J. Am. Chem. Soc.*, 1973, **95**, 5065–5067.

19 R. Paulini, K. Müller and F. Diederich, Orthogonal Multipolar Interactions in Structural Chemistry and Biology, *Angew. Chemie Int. Ed.*, 2005, **44**, 1788–1805.

20 F. H. Allen, C. A. Baalham, J. P. M. Lommerse and P. R. Raithby, Carbonyl{--}Carbonyl Interactions can be Competitive with Hydrogen Bonds, *Acta Crystallogr. Sect. B*, 1998, **54**, 320–329.

21 J. S. Murray and P. Politzer, σ-Holes and Si···N intramolecular interactions, *J. Mol. Model.*, 2019, **25**, 101.

22 J. Lu and S. Scheiner, *Mol.* , 2019, 24.

23 M. Liu, Q. Li, J. Cheng, W. Li and H. B. Li, Tetrel bond of pseudohalide anions with XH3F (X = C, Si, Ge, and Sn) and its role in SN2 reaction, *J. Chem. Phys.*, 2016, **145**, 224310.

24 Q.-Z. Li, H. Zhuo, H.-B. Li, Z. Liu, W. Li and J. Cheng, Tetrel–Hydride Interaction between XH 3 F (X = C, Si, Ge, Sn) and HM (M = Li, Na, BeH, MgH), *J. Phys. Chem. A*, 2015, **119**, 2217–2224.

25 R. C. Trievel and S. Scheiner, Crystallographic and computational characterization of methyl tetrel bonding in S-Adenosylmethionine-Dependent methyltransferases, *Molecules*, 2018, **23**, 1–17.

26 A. Daolio, P. Scilabra, G. Terraneo and G. Resnati, *Coord. Chem. Rev.*, 2020, 413, 213–265.

27 S. P. Thomas, M. S. Pavan and T. N. Guru Row, Experimental evidence for 'carbon bonding' in the solid state from charge density analysis, *Chem. Commun.*, 2014, **50**, 49–51.

28 V. Kumar, P. Scilabra, P. Politzer, G. Terraneo, A. Daolio, F. Fernandez-Palacio, J. S. Murray and G. Resnati, Tetrel and Pnictogen Bonds Complement Hydrogen and Halogen Bonds in Framing the Interactional Landscape of Barbituric Acids, *Cryst. Growth Des.*, 2021, **21**, 642–652.

29 G. Cavallo, P. Metrangolo, R. Milani, T. Pilati, A. Priimagi, G. Resnati and G. Terraneo, The halogen bond, *Chem. Rev.*, 2016, **116**, 2478–2601.

30 P. Scilabra, G. Terraneo and G. Resnati, The Chalcogen Bond in Crystalline Solids: A World Parallel to Halogen Bond, *Acc. Chem. Res.*, 2019, **52**, 1313–1324.

31 P. Scilabra, G. Terraneo and G. Resnati, Fluorinated elements of Group 15 as pnictogen bond donor sites, *J. Fluor. Chem.*, 2017, **203**, 62–74.

32 D. Mani and E. Arunan, The X–C···π (X = F, Cl, Br, CN) Carbon Bond, *J. Phys. Chem. A*, 2014, **118**, 10081–10089.

33 J. E. Del Bene, I. Alkorta and J. Elguero, Anionic complexes of F- and Cl- with substituted methanes: Hydrogen, halogen, and tetrel bonds, *Chem. Phys. Lett.*, 2016, **655–656**, 115–119.

34 S. K. Nayak, V. Kumar, J. S. Murray, P. Politzer, G. Terraneo, T. Pilati, P. Metrangolo and G. Resnati, Fluorination promotes chalcogen bonding in crystalline solids, *CrystEngComm*, 2017, **19**, 4955–4959.

35 C. Hansch, A. Leo and R. W. Taft, A survey of Hammett substituent constants and resonance and field parameters, *Chem. Rev.*, 1991, **91**, 165–195.

36 M. H. Nantz, L. Li, J. Zhu, K. L. Aho-Sharon, D. Lim and K. L. Erickson, Inductive electron-withdrawal from ammonium ion headgroups of cationic lipids and the influence on DNA transfection, *Biochim. Biophys. Acta - Lipids Lipid Metab.*, 1998, **1394**, 219–223.

37 A. Michrowska, Ł. Gułajski, Z. Kaczmarska, K. Mennecke, A. Kirschning and K. Grela, A green catalyst for green chemistry: Synthesis and application of an olefin metathesis catalyst bearing a quaternary ammonium group, *Green Chem.*, 2006, **8**, 685–688.

38 J.-X. Lin, A. Daolio, P. Scilabra, G. Terraneo, H. Li, G. Resnati and R. Cao, The Relevance of Size Matching in Self-assembly: Impact on Regio- and Chemoselective Cocrystallizations, *Chem. - A Eur. J.*, 2020, **26**, 11701–11704.

39 D. H. Malin, J. R. Lake, C. K. Schopen, J. W. Kirk, E. E. Sailer, B. A. Lawless, T. P. Upchurch, M. Shenoi and N. Rajan, Nicotine Abstinence Syndrome Precipitated by Central But Not Peripheral Hexamethonium, *Pharmacol. Biochem. Behav.*, 1997, **58**, 695–699.

40 S. R. Williams and L. N. Fletcher, A Dendritic Substrate for the Cholinergic Control of Neocortical Output Neurons, *Neuron*, 2019, **101**, 486-499.e4.

41 T. Sugino, J. Yamaura, M. Yamagishi, Y. Kurose, M. Kojima, K. Kangawa, Y. Hasegawa and Y. Terashima, Involvement of cholinergic neurons in the regulation of the ghrelin secretory response to feeding in sheep, *Biochem. Biophys. Res. Commun.*, 2003, **304**, 308–312.

42 T. J. Mooibroek, *Mol.* , 2019, 24.

43 S. Scheiner, Ability of IR and NMR Spectral Data to Distinguish between a Tetrel Bond and a Hydrogen Bond, *J. Phys. Chem. A*, 2018, **122**, 7852–7862.

44 A. Bauzá and A. Frontera, *Cryst.* , 2016, 6.

45 S. P. Thomas, M. S. Pavan and T. N. Guru Row, Experimental evidence for 'carbon bonding' in the solid state from charge density analysis, *Chem. Commun.*, 2014, **50**, 49–51.

46 S. Scheiner, Ability of IR and NMR Spectral Data to Distinguish between a Tetrel Bond and a Hydrogen Bond, *J. Phys. Chem. A*, 2018, **122**, 7852–7862.

47 A. Karim, N. Schulz, H. Andersson, B. Nekoueishahraki, A.-C. C. Carlsson, D. Sarabi, A. Valkonen, K. Rissanen, J. Gräfenstein, S. Keller and M. Erdélyi, Carbon's Three-Center, Four-Electron Tetrel Bond, Treated Experimentally, *J. Am. Chem. Soc.*, 2018, **140**, 17571–17579.

48 K. Akiba, Y. Moriyama, M. Mizozoe, H. Inohara, T. Nishii, Y. Yamamoto, M. Minoura, D. Hashizume, F. Iwasaki, N. Takagi, K. Ishimura and S. Nagase, Synthesis and Characterization of Stable Hypervalent Carbon Compounds (10-C-5) Bearing a 2,6-Bis(p-substituted phenyloxymethyl)benzene Ligand, *J. Am. Chem. Soc.*, 2005, **127**, 5893–5901.

49 D. Jayatilaka and B. Dittrich, X-ray structure refinement using aspherical atomic density functions obtained from quantum-mechanical calculations, *Acta Crystallogr. Sect. A*,

2008, **64**, 383–393.

50 M. Woińska, D. Jayatilaka, M. A. Spackman, A. J. Edwards, P. M. Dominiak, K. Woźniak, E. Nishibori, K. Sugimoto and S. Grabowsky, Hirshfeld atom refinement for modelling strong hydrogen bonds, *Acta Crystallogr. Sect. A*, 2014, **70**, 483–498.

51 W. Magdalena, G. Simon, D. P. M., W. Krzysztof and J. Dylan, Hydrogen atoms can be located accurately and precisely by x-ray crystallography, *Sci. Adv.*, 2021, **2**, e1600192.

52 L. A. Malaspina, E. K. Wieduwilt, J. Bergmann, F. Kleemiss, B. Meyer, M. F. Ruiz-López, R. Pal, E. Hupf, J. Beckmann, R. O. Piltz, A. J. Edwards, S. Grabowsky and A. Genoni, Fast and Accurate Quantum Crystallography: From Small to Large, from Light to Heavy, *J. Phys. Chem. Lett.*, 2019, **10**, 6973–6982.

53 E. K. Wieduwilt, G. Macetti, L. A. Malaspina, D. Jayatilaka, S. Grabowsky and A. Genoni, Post-Hartree-Fock methods for Hirshfeld atom refinement: are they necessary? Investigation of a strongly hydrogen-bonded molecular crystal, *J. Mol. Struct.*, 2020, **1209**, 127934.

54 A. Genoni, L. Bučinský, N. Claiser, J. Contreras-García, B. Dittrich, P. M. Dominiak, E. Espinosa, C. Gatti, P. Giannozzi, J.-M. Gillet, D. Jayatilaka, P. Macchi, A. Ø. Madsen, L. Massa, C. F. Matta, K. M. Merz Jr., P. N. H. Nakashima, H. Ott, U. Ryde, K. Schwarz, M. Sierka and S. Grabowsky, Quantum Crystallography: Current Developments and Future Perspectives, *Chem. – A Eur. J.*, 2018, **24**, 10881–10905.

55 S. Grabowsky, A. Genoni and H.-B. Bürgi, Quantum crystallography, *Chem. Sci.*, 2017, **8**, 4159–4176.

56 A. Genoni and P. Macchi, Quantum Crystallography in the Last Decade: Developments and Outlooks, *Crystals*, 2020, **10**, 473.

57 E. R. Johnson, S. Keinan, P. Mori-Sánchez, J. Contreras-García, A. J. Cohen and W. Yang, Revealing noncovalent interactions, *J. Am. Chem. Soc.*, 2010, **132**, 6498–6506.

58 J. Contreras-García, E. R. Johnson, S. Keinan, R. Chaudret, J.-P. Piquemal, D. N. Beratan and W. Yang, NCIPLOT: A Program for Plotting Noncovalent Interaction Regions, *J. Chem. Theory Comput.*, 2011, **7**, 625–632.

59 D. Arias-Olivares, E. K. Wieduwilt, J. Contreras-García and A. Genoni, NCI-ELMO: A New Method To Quickly and Accurately Detect Noncovalent Interactions in Biosystems, *J. Chem. Theory Comput.*, 2019, **15**, 6456–6470.

60 F. Peccati, NCIPLOT4 Guide for Biomolecules: An Analysis Tool for Noncovalent Interactions, *J. Chem. Inf. Model.*, 2020, **60**, 6–10.

61 J. Martí-Rujas, L. Meazza, G. K. Lim, G. Terraneo, T. Pilati, K. D. M. Harris, P. Metrangolo and G. Resnati, An Adaptable and Dynamically Porous Organic Salt Traps Unique Tetrahalide Dianions, *Angew. Chemie Int. Ed.*, 2013, **52**, 13444–13448.

62 L. Meazza, J. Martí-Rujas, G. Terraneo, C. Castiglioni, A. Milani, T. Pilati, P. Metrangolo and G. Resnati, Solid-state synthesis of mixed trihalides via reversible absorption of dihalogens by non porous onium salts, *CrystEngComm*, 2011, **13**, 4427.

63 G. M. Sheldrick, {\it SHELXT} {--} Integrated space-group and crystal-structure determination, *Acta Crystallogr. Sect. A*, 2015, **71**, 3–8.

64 A. L. Spek, Structure validation in chemical crystallography, *Acta Crystallogr. Sect. D*, 2009, **65**, 148–155.

65 D. Jayatilaka and D. J. Grimwood, in *Proceedings of the 2003 International Conference on Computational Science*, Springer-Verlag, Berlin, Heidelberg, 2003, pp. 142–151.

66 M. J. Frisch, G. W. Trucks, H. B. Schlegel, G. E. Scuseria, M. A. Robb, J. R. Cheeseman, G. Scalmani, V. Barone, B. Mennucci, G. A. Petersson, H. Nakatsuji, M. Caricato, X. Li, H. P. Hratchian, A. F. Izmaylov, J. Bloino, G. Zheng, J. L. Sonnenberg, M. Hada, M. Ehara, K. Toyota, R. Fukuda, J. Hasegawa, M. Ishida, T. Nakajima, Y. Honda, O. Kitao, H. Nakai, T. Vreven, J. A. Montgomery Jr., J. E. Peralta, F. Ogliaro, M. Bearpark, J. J. Heyd, E. Brothers, K. N. Kudin, V. N. Staroverov, R. Kobayashi, J. Normand, K. Raghavachari, A. Rendell, J. C. Burant, S. S. Iyengar, J. Tomasi, M. Cossi, N. Rega, J. M. Millam, M. Klene, J. E. Knox, J. B. Cross, V. Bakken, C. Adamo, J. Jaramillo, R. Gomperts, R. E. Stratmann, O. Yazyev, A. J. Austin, R. Cammi, C. Pomelli, J. W. Ochterski, R. L. Martin, K. Morokuma, V. G. Zakrzewski, G. A. Voth, P. Salvador, J. J. Dannenberg, S. Dapprich, A. D. Daniels, Ö. Farkas, J. B. Foresman, J. V Ortiz, J. Cioslowski and D. J. Fox, .

67 F. Cortés-Guzmán and R. F. W. Bader, Complementarity of QTAIM and MO theory in the study of bonding in donor–acceptor complexes, *Coord. Chem. Rev.*, 2005, **249**, 633–662.

68 T. A. Keith, AIMAll, Version 13.11.04; TK Gristmill Software: Overland Park, KS, USA, 2012; available online: aim.tkgristmill.com.

69 E. Espinosa, E. Molins and C. Lecomte, Hydrogen bond strengths revealed by topological analyses of experimentally observed electron densities, *Chem. Phys. Lett.*, 1998, **285**, 170–173.

70 M. D. Esrafili, S. Asadollahi, P. Mousavian, Anionic tetrel bonds: An ab initio study, *Chem. Phys. Lett.*, 2018, **691**, 394-400.

71 E. Bartashevich, Y. Matveychuk and V. Tsirelson, Identification of the Tetrel Bonds between Halide Anions and Carbon Atom of Methyl Groups Using Electronic Criterion, *Molecules*, 2019, **24**, 1083.

72 S. J. Grabowski, Tetrel bond-σ-hole bond as a preliminary stage of the SN2 reaction, *Phys. Chem. Chem. Phys.*, 2014, **16**, 1824–1834.

73 D. Mani and E. Arunan, The X-C⋯Y (X = O/F, y = O/S/F/Cl/Br/N/P) 'carbon bond' and hydrophobic interactions, *Phys. Chem. Chem. Phys.*, 2013, **15**, 14377–14383.

74 V. R. Mundlapati, D. K. Sahoo, S. Bhaumik, S. Jena, A. Chandrakar and H. S. Biswal, Noncovalent Carbon-Bonding Interactions in Proteins, *Angew. Chemie - Int. Ed.*, 2018, **57**, 16496–16500.

